CRITICAL MOVEMENT OF LARGE ROCKS IN CURRENTS AND WAVES

by L.C. van Rijn;

(published by International Journal of Sediment Research, January 2019)

Prof. (retired); LVR-Sediment Consultancy; Domineeswal 6, 8356DS Blokzijl, The Netherlands; info@leovanrijn-sediment.com

Abstract

Cobbles, boulders, and rocks often are used in a bed protection layer near a structure to protect the underlying sand bed against erosion by combined current and waves. The design of a bed protection layer consisting of loose rocks (rubble mound) requires knowledge of the stability and movement (as bed load) of very coarse materials. If some movement (or damage) is acceptable, the rock diameter can be designed to be smaller. This paper addresses the stability and movement of very coarse materials (cobbles, boulders, and rocks) based on the concept of the critical Shields mobility number. It is shown that the bed load transport of large cobbles, boulders, and rocks can be described by the equations of Meyer-Peter and Mueller (MPM) and Cheng. Both are valid for relatively small Shields mobility numbers. New and general equations for the design of a bed protection layer (including some permissible damage) in conditions with a current with or without waves are proposed based on the Shields mobility parameter and the bed load transport equation of Cheng. Laboratory and field data of critical velocities for pebbles, cobbles, boulders, and rocks have been analyzed and compared to the computed results of the proposed equations. Practical applications are given to demonstrate the general applicability of the proposed equations.

Keywords: Rock stability, Bed protection, Critical movement, Bed load transport, Rocks

1. Introduction

Cobbles, boulders, and rocks often are used as a protection layer near a structure to protect the underlying sand bed against erosion by current and waves. Some examples are: (1) rock protection around monopiles of windmills; (2) rock protection at the bed near harbor quay walls against ship propeller scour; (3) rock cover of pipelines against the impact of anchors and (4) rock berm at the toe of breakwaters.

The stability of coarse materials in conditions with current and/or waves has been studied extensively during the last 50 years. The Shields' (1936) curve related to the stability of loose materials in a current and the Hudson-formula (Hudson, 1958, CIRIA/CUR/CETMEF, 2007) for the stability of sloping rocks in coastal waters with waves are well known. Most research on bed protection has been done for currents. Simple expressions for uniform flow conditions without waves are given by Neill (1968), Maynord (1978) and Pilarczyck (1998). Hofland (2005) has studied the stability of rocks in non-uniform flows with relatively high turbulence levels by introducing a stability parameter based on the turbulent kinetic energy (k) in addition to the local mean velocity ($\overline{u}$). Much less research has been done on bed protection in coastal waters. Recent efforts are those of van den Bos et al. (2010) and Tørum et al. (2010) focussing on the transport of coarse materials at low mobility numbers based on the Paintall (1971) approach. An overview of research efforts and equations involved is given by Schiereck and Verhagen (2016). It is noted that many equations in the literature are (ad-hoc) equations which are only valid for the test conditions studied (mostly small-scale flumes). Using these formulae for prototype conditions, may introduce upscaling errors.

The design of a bed protection layer consisting of rocks (rubble mound) requires knowledge of the stability and movement of very coarse granular materials. Two types of bed protection can be designed: static or dynamic. A static bed protection means that the rocks are fully stable under design conditions without any damage/movement. A dynamic bed protection is obtained if some movement (or damage) is acceptable allowing use of smaller rock sizes.

This paper addresses the stability and movement of very coarse materials (cobbles, boulders, and rocks) based on the concept of the critical Shields (1936) mobility number related to a prescibed damage level. The damage parameter can be derived from the bed load equation of Cheng (2002), which is valid for relatively small Shields mobility numbers. New and general equations for the design of the rock size of a protection

layer (including allowance for damage/movement) in conditions with a current with or without waves are proposed. Many existing data sets have been analyzed focusing on cobbles, boulders, and rocks. It is shown that the new equations are valid for large-scale materials in both current and wave conditions in different situations. Practical applications are given to demonstrate the applicability of the new equations.
The novel aspects of this paper are: (i) compilation of field data of critical velocities for large cobbles, boulders, and rocks in the range of 0.03 to 3 m in both current and wave conditions, (ii) validation of bed load transport equations for these materials; and (iii) derivation of general equations for the design of bed protection including an estimate of the damage (loss of rocks) for given conditions.

2. Critical bed-shear stress and velocity for large rocks and cobbles

2.1. General

Critical movement of large cobbles, boulders, and rocks is related to the problem of initiation of movement, which was studied by Shields (1936) and others. The stability of these materials on a horizontal or mild sloping bottom in a current can be described by the method of Shields (1936) for granular material (Shields' curve). A drawback of this method is that the value of the friction coefficient is required which introduces additional uncertainty. The friction coefficient includes the effective roughness height (k_s) of Nikuradse (Nikuradse 1932, 1933; Van Rijn 2011), which is determined by the larger diameters of the size distribution ($k_s \cong D_{90}$; where D_{90} = diameter for which 90 percent of the material is finer). Assuming $D_{90} \cong 1.5$ to 2 D_{50} for narrowly graded materials, the k_s-value can be related to the median size, D_{50}: $k_s = \alpha D_{50}$ with α = 1.5 to 2, as used by many practitioners/engineers.
The size distribution of cobbles, boulders, or rocks can be determined by: (i) measuring (image analysis), (ii) sieving, and/or (iii) weighing. Based on measuring or sieving methods, the median size (D_{50}) can be found. Based on weighing of individual units, the mass distribution is obtained which can be converted to a spherical diameter $D_{s50} = [M_{50}/(0.166\ \pi\ \rho_s)]^{1/3}$ or a nominal diameter $D_{n50} = (M_{50}/\rho_s)^{1/3}$ where M_{50} = median mass, and ρ_s = density of sediment (rock). Herein, it is assumed: $D_{50} \cong D_{s50} \cong 1.2\ D_{n50}$ (see also Verhagen & Jansen, 2014).

2.2. Critical Shields mobility parameter

The basic problem of initiation of motion of granular materials due to a flow of water (without waves) has been studied by Shields (1936) and others. Based on theoretical work of the forces acting at a spherical particle and experimental work with granular materials in flumes, Shields (1936) proposed the classical Shields' curve for the stability of granular materials in a current.
The Shields' curve expresses the critical dimensionless shear stress also known as the critical Shields' mobility number ($\theta_{cr,shields}$) as function of a dimensionless particle-related Reynolds' number, as follows:

$$\theta_{cr,shields} = \frac{\tau_{b,cr}}{[(\rho_s-\rho_w)g\ D_{50}]} = \frac{\rho_w\ u_{*,cr}^2}{[(\rho_s-\rho_w)g\ D_{50}]} = \frac{u_{*,cr}^2}{[(s-1)g\ D_{50}]} = function(\frac{u_{*,cr}D_{50}}{\vartheta}) \quad (1)$$

where
$\tau_{b,cr} = \rho_w\ (u_{*cr})^2$ = critical bed-shear stress at initiation of motion,
u_{*cr}= critical bed-shear velocity,
ρ_w = density of water,
ν= kinematic viscosity coefficient of water.

The Shields' curve represents the transition from a state of stability to instability of granular material. Granular material is stable if:

$$\theta \le \theta_{cr} \quad \text{or} \quad \frac{\tau_b}{[(\rho_s-\rho_w)gD_{50}} \le \theta_{cr} \quad (2)$$

where τ_b = bed-shear stress.
Based on existing research papers on the inititiation of motion for fine cohesionless sediment particles in the range of 10 to 400 μm in the laminar and the turbulent flow range and the work of Soulsby (1997), the following equation for the critical bed-shear stress related to the initiation of motion for a horizontal bed is proposed:

$$\theta_{cr,shields} = \frac{0.3}{(1+D_*)} + 0.055[1 - \exp(-0.02D_*)] \qquad for\ D_* > 0.1 \qquad (3)$$
$$D_* = D_{50}\,[\frac{(s-1)g}{\vartheta^2}]^{1/3}$$

where: s = ρ_s/ρ_w = specific gravity of sediment.
The $\theta_{cr,shields}$-value of coarse materials > 10 mm is approximately constant at $\theta_{cr,shields} \cong 0.05$ (independent of the Reynolds' number; right part of the Shields' curve).
The data of the Shields' curve shows considerable scatter (spread of the data), which is caused by experimental errors, the precise definition of particle motion, differences between initial and final particle size, particle shape, and particle arrangement. It is well known that the particle arrangement at the start of the tests is very different from that at the end of the tests. The flow rearranges the grains in a way that they reach positions of maximum resistance to movement. Furthermore, the precise definition of initiation of motion used by Shields is not very clear. Experimental research at Deltares (1972) based on visual observations shows that the Shields' curve actually represents a state with weak to frequent movement of particles. For design purposes, it is most practical to use a lower envelope curve. In the current paper, this lower envelope is represented by a correction/reduction coefficient (r).
The precise critical mobility parameter of a single coarse particle at the threshold of movement is herein defined as: $\theta_{cr} = r\,\theta_{cr,shields}$ with $\theta_{cr,shields} = 0.05$; r = reduction coefficient in the range of 0.4 to 1.
The reduction coefficient (r) from the relationship $\theta_{cr} = r\,\theta_{cr,shields}$ can be seen as a correction parameter acting on the Shields' curve to define a particular stage of movement (or damage).

Based on visual observations during the initiation of motion experiments of Deltares (1972), the r-parameter is herein defined, as follows:

r = 0.4 (occasional particle movement at some locations; ≅ 0.1% of surface is moving);
r = 0.6 (frequent particle movement at some locations; ≅ 1% of surface is moving);
r = 0.8 (frequent particle movement at many locations; ≅ 10% of surface is moving);
r = 1.0 (frequent particle movement at nearly all locations; ≅ 50% of surface is moving).

In the case of a sloping bed, the θ_{cr}-value can be computed as:

$$\theta_{cr} = K_{\alpha 1}\, K_{\alpha 2}\, r\, \theta_{cr,shields} \qquad (4)$$

$$K_{\alpha 1} = \frac{\sin(\varphi - \alpha_1)}{\sin\varphi} \quad and \quad K_{\alpha 2} = \cos\alpha_2\,[1 - \frac{(\tan\alpha_2)^2)}{(\tan\varphi)^2}]^{0.5}$$

where
$K_{\alpha 1}$ = slope factor (longitudinal slope,
K = 1 for horizontal bed, see van Rijn 1993, 2006);
$K_{\alpha 2}$ = slope factor (lateral slope ,
K = 1 for horizontal bed, see van Rijn 1993);
α_1= angle of longitudinal slope; α_2 = angle of lateral slope;
φ = angle of repose (30 to 40 degrees).

The Shields' curve (Eq. 3) is also valid for conditions with current plus waves, provided that the bed-shear stress due to current and waves ($\tau_{b,cw}$) is computed as (van Rijn 1993):

$$\tau_{b,cw} = \tau_{b,c} + \tau_{b,w} \qquad (5)$$

where:

$\tau_{b,c} = 0.125\, \rho_w\, f_c\, (\gamma_{str}\, u_c)^2$ = bed-shear stress due to current (N/m^2)

$\tau_{b,w} = 0.25\, \rho_w\, f_w\, (\gamma_{str}\, U_w)^2$= bed-shear stress due to waves (N/m^2);

$U_w = \frac{\pi H_s}{T_p \sinh(\frac{2\pi h}{L_s})}$ = near-bed peak orbital velocity based on linear wave theory (m/s);

$f_c = \frac{0.24}{[\log(12h/k_s)]^2}$ = current-related friction factor for rough flow regime (cobbles and rocks are in the hydraulic rough regime as viscous sublayer effects cannot develop);

$f_w = \exp\{-6 + 5.2(A_w/k_s)^{-0.19}\}$ = wave-related friction factor for rough regime;

u_c= depth-averaged current velocity (m/s);
U_w = near-bed peak orbital velocity (m/s) = $\pi\, H_s T_p^{-1}[\sinh(2\pi h/L_s)]^{-1}$ (linear wave theory);
γ_{str} = velocity+turbulence enhancement factor due the presence of a structure (-);
f_c = $0.24[\log(12h/k_s)]^{-2}$= current-related friction factor for rough flow regime (cobbles and rocks are in the hydraulic rough regime as viscous sublayer effects cannot develop);
f_w= $\exp\{-6 + 5.2(A_w/k_s)^{-0.19}\}$= wave-related friction factor for rough regime;
h = water depth (m);
H_s = significant wave height (m); L_s = significant wave length (m);
T_p = wave period of peak of wave spectrum (s);
$A_w = (0.5T_p/\pi)U_w$ = near-bed peak orbital amplitude;
k_s= effective bed roughness of Nikuradse; ($k_s = \alpha\, D_{50}$ and α= 1.5 to 2 for narrowly graded stones/rocks, see Section 2.1).

Using the Shields' concept, the friction factors have to be known. The commonly used friction factors f_c and f_w are not practical, because they involve iterative computations. Therefore, approximate power functions $f_{c,a} = 0.11(h/k_s)^{-0.3}$ = current-related friction factor (-) and $f_{w,a} = 0.1(A_w/k_s)^{-0.3}$ = wave-related friction factor (-) are introduced to obtain a simple and explicit solution in the most general case of combined current and wave conditions. This approach implies a slightly less accurate solution, but provides the benefit of simplicity. Furthermore, this approach yields simple expressions explicitly showing the most basic influencing parameters.

To justify the use of the approximation functions, both parameters ($f_{c,a}$ and $f_{w,a}$) are compared to the traditional methods (f_c and f_w) in Table 1 for relative roughness parameters $h/(\alpha D_{50})$ and $A_w/(\alpha D_{50})$ in the practical range of 10 to 300 for coarse granular materials. The current-related approximation function $f_{c,a}$ is quite accurate compared to f_c, but the wave-related approximation function $f_{w,a}$ is somewhat less accurate compared to f_w. It is noted that the application of the approximation functions $f_{c,a}$ and $f_{w,a}$ is not essential. The more precise f_c and f_w can also be used in Eq. 6, but the solution requires an iterative solution method.

Table 1. Current-related and wave-related friction factors

Relative roughness $h/(\alpha D_{50})$; $A_w/(\alpha D_{50})$ (-)	Current-related friction			Wave-related friction	
	Chézy coefficient C ($m^{0.5}/s$)	friction factor $f_c=8g/C^2$ (-)	approximate friction factor $f_{c,a}=0.11[h/(\alpha D_{50})]^{-0.3}$ (-)	friction factor f_w (-)	approximate friction factor $f_{w,a}=0.1[A_w/(\alpha D_{50})]^{-0.3}$ (-)
10	37.4	0.056	0.055	0.071	0.050
15	40.6	0.048	0.049	0.055	0.044
20	42.8	0.043	0.045	0.047	0.041
50	50.0	0.031	0.034	0.029	0.031
100	55.4	0.026	0.028	0.022	0.025
150	58.6	0.023	0.024	0.018	0.022
200	60.8	0.021	0.022	0.017	0.020
300	64.1	0.02	0.020	0.014	0.018

$C=5.75g^{0.5}\log(12h/(\alpha D_{50}))$= Chézy coefficient

2.3. Stability equations for coarse materials in currents plus waves

The most general case is the stability of coarse materials in conditions with current plus waves. Using the available Equations 3, 4, and 5, the critical diameter of coarse materials can be expressed as:

$$D_{50} = \frac{\tau_{b,cw}}{[(\rho_s - \rho_w)\, g\, (K_{\alpha 1}\, K_{\alpha 2}\, r\, \theta_{cr,shields})]} \quad (6)$$

where $\tau_{b,cw}$ = shear stress at the granular material due to current plus waves (see Eq. 5).
Using the approximation functions $f_{c,a}$ and $f_{w,a}$, Eq. 6 can be expressed as:

$$D_{50} = \frac{\gamma_s[0.013\left(\frac{h}{\alpha}\right)^{-0.3}(\gamma_{str}\, u_c)^2 + 0.045\left(\frac{Tp}{\alpha}\right)^{-0.3}(\gamma_{str}\, U_w)^{1.7}]^{1.4}}{[(s-1)\, g\, K_{\alpha 1}\, K_{\alpha 2}\, r\, \theta_{cr,shields}]^{1.4}} \quad (7)$$

where: α = bed roughness coefficient ($k_s = \alpha D_{50}$ with α = 1.5 to 2);
γ_s = safety factor;
u_c= depth-averaged current velocity (m/s);
U_w = near-bed peak orbital velocity (m/s) = $\pi H_s T_p^{-1}[\sinh(2\pi h/L_s)]^{-1}$ (linear wave theory);
γ_{str} = velocity+turbulence enhancement factor due the presence of a structure (-);
h = water depth (m);
H_s = significant wave height (m); L_s = significant wave length (m);
T_p = wave period of peak of wave spectrum (s);
$A_w = (0.5T_p/\pi)U_w$ = near-bed peak orbital amplitude;
k_s= effective bed roughness of Nikuradse;
$s = \rho_s/\rho_w$=relative density;
$K_{\alpha 1}$ = slope factor (longitudinal slope; K = 1 for horizontal bed, see van Rijn 1993, 2006);
$K_{\alpha 2}$ = slope factor (lateral slope; K = 1 for horizontal bed, see van Rijn 1993);
α_1= angle of longitudinal slope; α_2 = angle of lateral slope;
φ = angle of repose (30 to 40 degrees);
$\theta_{cr,shields}$ = critical Shields parameter (=0.05 for coarse sediment);
r = reduction coefficient of critical Shields parameter (0.4 to 1).

Equation 7 is also valid for currents alone (U_w= 0) or for waves alone (u_c= 0). Finally, it is noted that the critical condition for initiation of motion is affected by the water depth (see Eq. 7), which is also discussed by Cheng et al. (2016).
The three most important input coefficients to be determined are α, r, and γ_{str}. The γ_{str}-coefficient can also be expressed in terms of the standard deviation (σ_u) of the velocity, as follows: $\gamma_{str}\, u_c = u_c + n\, \sigma_u$. Using: $\sigma_u = \gamma\, u_c$, it follows that: $\gamma_{str} = 1 + n\, \gamma$, with n = 2 to 3 and γ = 0.2 to 0.3 resulting in γ_{str} = 1 to 2.

2.4. Comparison of measured and computed critical velocities of large cobbles, boulders, and rocks

2.4.1. General

Most of the research on initiation of motion of particles is related to relatively small particles with diameters < 10 mm in laboratory flumes (see Shields, 1936; Graf, 1971; Yalin, 1977; van Rijn, 1993; Soulsby, 1997; and will not be discussed here. In this paper, the attention is focused on critical conditions of large size cobbles, boulders, and rocks focussing on field data. Although field data on the (critical) movement of large cobbles, boulders, and rocks are scarce, a small set of data could be compiled (Table 2) which is discussed hereafter.

2.4.2. Currents

Atal and Lavé (2009) have studied the movement of pebbles and rocks with diameters in the range of 5 to 70 mm in a laboratory flume. Pebbles moved by saltation and occasionally by rolling. Mean saltation velocities during the saltations (hops) were measured directly from particle tracking. The critical velocities are roughly: $u_{critical}$ = 1 m/s for D_{50} = 15 mm to $u_{critical}$ = 1.75 m/s for D_{50} = 70 mm, see Table 2.
Helley (1969) has studied the threshold velocities of large size rocks (0.15 to 0.45 m) in the Blue Creek mountain river (U.S.). Natural rocks of various sizes and shapes were painted fluorescent red, tagged by a float and placed at the bed of the creek. Near-bed velocities were measured close to the tagged rocks. The water depth was in the range of 1 to 1.2 m. Initiation of motion was defined as the sudden movement of the floats. Helley (1969) also presents the field data of similar measurements by Fahnestock (1963), see Table 2.
Inbar and Schick (1979) have studied the critical movement of boulders and rocks during flash floods in the upper Jordan River and the Meshushim River in Israel (see also Section 3). An extreme rainstorm in January 1969 generated a flood in the Jordan River. Boulders up to 1.3 m were moved, and the channel was completely reshaped. During the same event, a 300 m^3/s peak flow occurred in the neighboring Nahal Meshushim River. Here too, numerous boulders of 1 m diameter were transported. The critical flow velocities in depths of 1 to 1.5 m can be summarized, as follows: $u_{critical}$ = 2-2.5 m/s, for D_{50} = 0.25-0.5 m and $u_{critical}$ = 2.5-3 m/s for D_{50} = 0.5-1 m, see Table 2. Turowski et al. (2009) have studied the movement of boulders and rocks in the Erlenbach mountain stream (Switzerland). Boulders with median diameters of up to 1.35 m and estimated weights of more than 2.5 tons were observed to move during extreme events. Boulders of about 0.5 to 0.65 m were found to be fully mobile in peak flow conditions with mean velocities of about 3 m/s (discharge of about 15 m^3/s, mean flow width of 4 m and mean flow depth of 1.2 m).
Mueller et al. (2005) have studied the threshold bed-shear stress (θ_{cr}) of bed-load transport of coarse materials with D_{50}-values in the range of 0.025 to 0.21 m in various mountain streams (Idaho, U.S.). The θ_{cr}-value is related to a very small dimensionless reference bed-load transport rate of 0.002. Analysis of their data shows that the critical Shields-parameter varies considerably in the range of 0.01 to 0.12, which is a much wider range than the laboratory range of 0.02 to 0.06. Based on this field data set, the movement of cobbles/boulders/rocks is possible at very low mobility values of 0.01 to 0.02. It is found that the ratio D_{50}/D_{90} has a clear effect on the θ_{cr}-value. This ratio expresses the grading of the bed material; a small value means a wide grading resulting in hiding-exposure effects. Smaller rocks/fragments are more difficult to mobilize, as they are hiding between the larger rocks. Another parameter of importance is the variation of the ratio h/D_{50} with h= water depth. Rocks are more difficult to move in the case of small submergence (h/D_{50} is small), because the flow resistance is relatively large and the near-bed velocities are relatively small.

All available data of cobbles and rocks are summarized in Table 2 and in Fig. 1. The uncertainty range of particle size and critical velocity is about 10% for the flume data and 15% to 20% for the field data. It is noted that the field data with large rock sizes up to 0.7 m refer to very shallow mountain rivers with depths in the range of 0.5 to 1.2 m ($h/D_{50} < 10$). This type of flow is generally known as the "wild" water regime at steep slopes (see also Table 4) with exceptionally high turbulence levels exceeding those of normal open channel flow ($h/D_{50} > 100$). Furthermore, the field data tests of relatively large rocks concern the initiation of motion of very isolated rocks which are placed on top of the river bed and are, thus, extremely exposed to the local turbulent velocities. This test arrangement is very different from a bed protection layer consisting of rocks of approximately the same size with sheltering effects due to the presence of neighboring rocks.

Equation 7 has three input parameters: α-coefficient related to bed-roughness effect (range 1 to 2), r-coefficient related to the most appropriate critical Shields mobility number range (range 0.3 to 0.5), and the γ_{str}-coefficient related to the velocity and turbulence enhancement due to the bed-structure arrangement (range 1 to 1.6). The α-coefficient is set to α=2, which means that the effective bed roughness is equal to $k_s = 2D_{50} \cong D_{90}$. The other two coefficients have been varied to fit the data of Fig. 1. Computed results are shown for r = 0.3, 0.4, and 0.5 and γ_{str} = 1.2 in Fig. 1. The latter coefficient (γ_{str}) represents the effect that the rocks used in field tests are isolated rocks fully exposed to the flow with extreme turbulence levels. Fairly reasonable agreement between measured and computed results can be observed for r= 0.4 in combination with γ_{str}= 1.2 (regression coefficient $R^2 \cong 0.8$). The curve for r = 0.4 passes through most of the uncertainty ranges of the measured data.

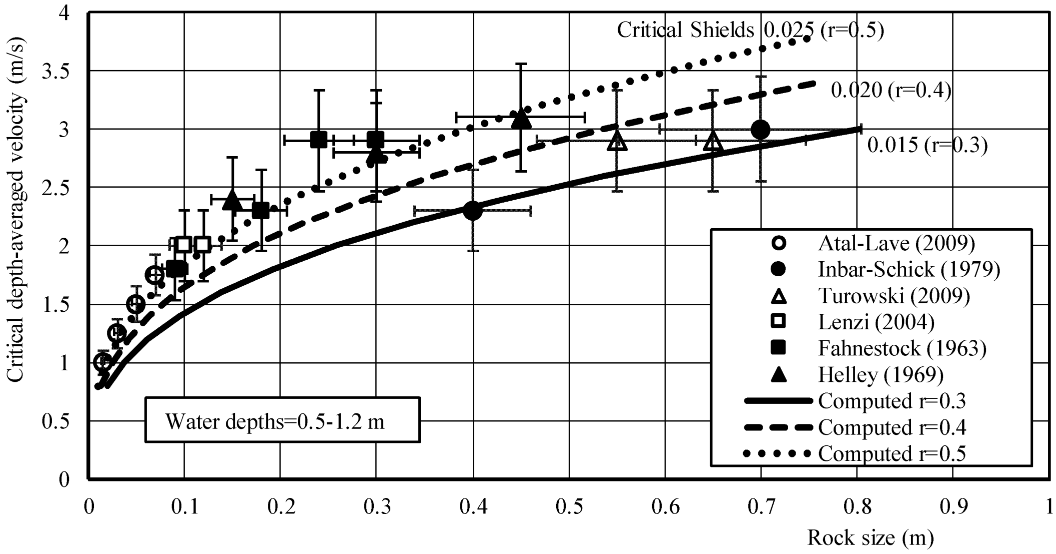

Fig. 1. Critical depth-averaged velocity as a function of rock size in a current (γ_{str} = 1.2)

Table 2. Summary of critical conditions for large size particles/rocks in current conditions

Data set	Water depth (m)	Particle/rock size (m)	Critical depth-mean velocity (m/s)
Flume: Atal and Lavé (2009)	<0.5	0.015; 0.03; 0.05; 0.07	1.0; 1.25; 1.5; 1.75
Field: Inbar and Schick (1979)	1-1.2	0.4; 0.7	2.3; 3.0
Field: Turowski et al. (2009)	0.5-1	0.6	3.0
Field: Lenzi (2004), Lenzi et al. (2006), Mao and Lenzi (2007), Rainato et al. (2017)	<0.5	0.11	2.0
Field: Fahnestock (1963)	0.5-1	0.09; 0.18; 0.24; 0.3	1.8; 2.3; 2.9; 2.9
Field: Helley (1969)	1-1.2	0.15; 0.3; 0.45	2.4; 2.8; 3.1

2.4.3. Waves

Field data on the stability of cobbles, boulders, and rocks in coastal seas are extremely scarce, as such studies require (expensive) field surveys in harsh sea conditions.

Crickmore et al. (1972) of Hydraulics Research Wallingford have performed a pebble tracer experiment in the English Channel east of Portsmouth. The local seafloor consists of natural pebbles. The peak tidal velocities are 0.5 m/s during neap tide and 0.8 m/s during spring tide. Radioactive tagged pebbles (D_{50} = 28 mm, D_{min} = 19 mm, D_{max} = 38 mm) were placed by divers at three areas (30x60 m^2) with depths of 9, 12, and 18 m (about 1000 tagged pebbles at each area). The site is exposed to waves from south-west to south-east. Wave records were obtained at the Owers light vessel at a depth of about 25 m (about 25 km south-west from the pebble areas). Tracer displacement was measured by towing a detection instrument behind the survey vessel. The inaccurary of the horizontal positioning system was estimated to be about 5 to 10 m. The thickness of the upper bed layer in which tagged particles were observed, was in the range of 60 to 120 mm. Various storms occurred during the observation period. The maximum significant wave height was about $H_{s,max}$ = 5 m in depth of 18 m reducing to $H_{s,max}$ = 3 m in a depth in 9 m and wave periods of 8 to 10 s. The pebble movement was about 40 m at the site with a depth of 9 m, about 15 m at a depth of 15 m and zero at a depth of 18 m. Table 3 (Row 1) lists the measured results for the site with a depth of 18 m.
Based on this, the critical peak orbital velocity of pebbles with D_{50} = 0.028 m is estimated to be $U_{w,cr} \cong 1.2$ m/s. Equation 7 yields similar results for $r \cong 0.5$, s = 2.6, γ_{str} = 1 (no structure), T_p = 8 s, α = 2, see Fig. 2 (most left data point). This corresponds to a critical mobility number of $\theta_{cr} \cong 0.025$, which is much lower than the standard critical Shields value of $\theta_{cr,shields}$ = 0.05.

Hall (2010) and Hansom et al. (2008) have studied the movement of individual natural boulders in conditions with breaking waves at the shore platform of East Lothian on the high-energy, macro-tidal North Sea coast of Scotland. Boulders with volumes of more than 0.5 m^3 were observed to move landward over extensive areas of the shore platform. The velocity in breaking waves was estimated to have reached values of 3 to 4 m/s on the platform, especially in the sligthly deeper channels eroded at the platform floor. Sliding is the dominant mechanism of movement for irregular shaped (mega) clasts. Rolling and overturning processes occur for platy clasts. Boulder sizes and estimated critical velocities related to boulder sliding are listed in Table 3 (rows 2-10) and shown in Fig. 2.

Table 3. Summary of critical conditions for large size particles/rocks in wave conditions

Sediment size		**Type of material**	**Density**	**Water depth**	**Estimated critical velocity for sliding and rolling**
Range (m)	**Mean (m)**		**(kg/m³)**	**(m)**	**(m/s)**
0.019-0.038	0.028	quartz	2650	9-18	1.2
0.14-0.27	0.2	agglomerate	2360	2-4	2.1
0.16-0.48	0.3	sandstone	2550	2-4	2.2
0.22-0.73	0.45	sandstone	2550	2-4	3.4
0.33-1.25	0.75	agglomerate	2360	2-4	3.7
0.8-1.15	1.0	basalt	3040	2-4	4.9
0.59-1.59	1.1	basalt	3040	2-4	5.5
1.07-2.1	1.5	sandstone	2550	2-4	5.7
0.74-2.51	1.6	basalt	3040	2-4	6.4
1.23-3.05	2.0	basalt	3040	2-4	6.9

Equation 7 has been used to compute the critical peak orbital velocity for the boulder sizes listed in Table 3 using: ρ_w = 1020 kg/m^3, α = 1, r= 0.3, 0.4, and 0.5 and γ_{str} = 1.2. This latter coefficient represents the effect that the boulders at the field site are isolated rocks fully exposed to breaking waves with extreme turbulence levels.
Computed results are shown in Fig. 2 for r = 0.3, 0.4, and 0.5 and γ_{str} = 1.2. Fairly good agreement between measured and computed results can be observed for r = 0.4 and r = 0.5 in combination with γ_{str} = 1.2. These settings also yield the best results for rocks in a current (see Fig. 1).

Based on Figs. 1 and 2, it is concluded that the stability Eq. 7 yields fairly good results in predicting the stable rock size for both current and wave conditions using the same settings of the two most important input coefficients (r and γ_{str}). To estimate the loss of rocks from a bed protection system for conditions just above critical conditions, the bed load transport of rocks should be known, which is discussed in the following section.

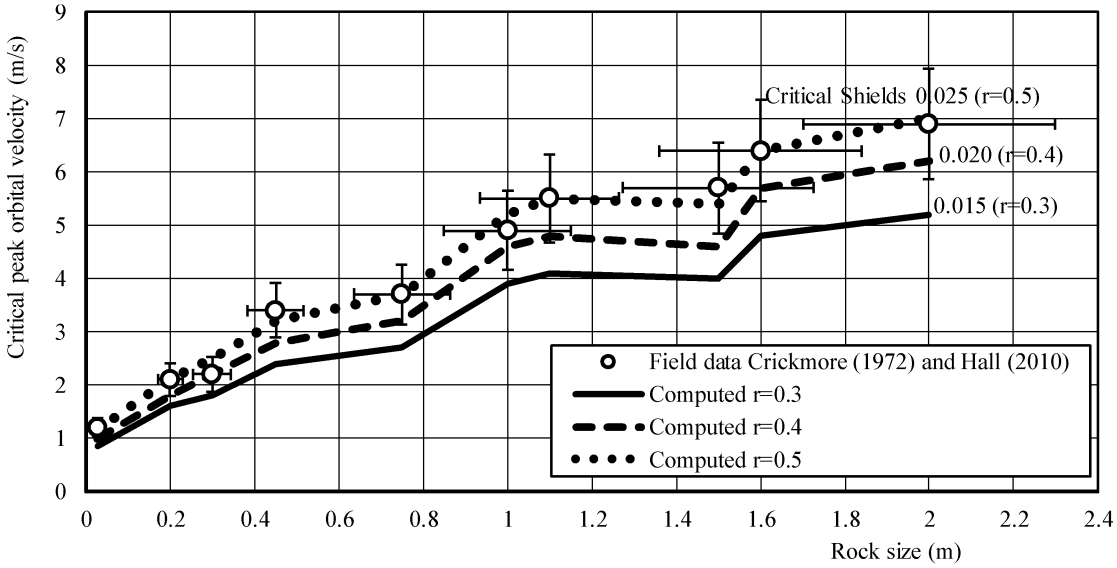

Fig. 2. Critical peak orbital velocity as a function of rock size in waves (γ_{str} = 1.2)

3. Bed load transport of rocks at low bed-shear stresses

3.1. Bed load transport equations

In this section it is shown that the bed load transport equations of Meyer-Peter and Mueller (MPM) (1948) and Cheng (2002) can be used to determine the bed load transport of large size cobbles and rocks at low values of the bed shear stress. The equation of MPM reads, as follows:

$$\varphi_b = 8\,(\theta - \theta_{cr})^{1.5} \tag{8}$$

$$\varphi_b = \frac{q_{b,mass}}{\rho_s\, g^{0.5}\,(s-1)^{0.5}\, D_{50}^{1.5}} = \text{dimensionless bed load transport}$$

$$\theta = \frac{\tau_b}{(\rho_s-\rho_w)\, g\, D_{50}} = \text{dimensionless mobility parameter (Shields-parameter)}$$

where
φ_b = dimensionless bed load transport;
θ = dimensionless mobility parameter (Shields-parameter); θ_{cr} = 0.047 (-);
$q_{b,mass}$ = bed load transport by mass (kg/(m s));
$\tau_b = 0.125\rho_w f_c\,[u_c]^2$ (N/m^2),

u_c = depth-averaged velocity (m/s) and
f_c = grain-related Chézy-coefficient = $0.11(h/\alpha D_{50})^{-0.3}$.

The original MPM-equation is valid for $\theta_{cr} = 0.047$.

The bed-load transport equation of Cheng (2002) can also be used for very coarse materials and is given by

$$\varphi_b = 13\,\theta^{1.5}\exp(\frac{-0.05}{\theta^{1.5}}) \quad (9)$$
$$q_b = 13\,\rho_s\,(s-1)^{0.5} g^{0.5} D_{50}^{1.5}\,\theta^{1.5}\exp\left(\frac{-0.05}{\theta^{1.5}}\right)$$

Equation 9 has no threshold value. At high θ-values, the bed load transport approaches to $\varphi_b = 13\,\theta^{1.5}$.

3.2. Measured bed load transport of cobbles, boulders, and rocks

The knowledge of bed load transport of large size rocks at low bed-shear stresses in field conditions is rather limited. Some laboratory data are available (Meyer-Peter and Mueller, 1946; Paintal, 1971 and others). Herein, both flume and field data of relatively coarse materials have been used to study bed load transport at low shear stresses.
A subset of the flume data of Meyer-Peter and Mueller (1948) focussing on the most coarse gravel materials among their experiments has been reanalyzed and plotted in Fig. 3. The particle sizes are D_{50} = 28 mm and 5.2 mm. The water depths vary in the range of 0.06 m in the narrow flume (width = 0.35 m) up to 1.09 m in the wide flume (width = 2 m). The cross section-averaged velocities are in the range of 0.85 to 2.85 m/s. Fig. 3 shows the dimensionless bed load transport rate, ϕ_b, as a function of the grain-related Shields parameter θ. An important contribution to the study of the stability of coarse granular material has been made by Paintal (1971), who has measured the dimensionless (bed load) transport of granular material at conditions with θ-values in the range of 0.01 to 0.04. The data of Paintal covering this range of θ=0.01 to 0.04 also are shown in Fig. 3.
Reliable field data of large cobbles, boulders and rocks are extremely scarce. Only three field data sets have been found: Rio Cordon in Italy (Lenzi, 2004; Lenzi et al., 2006; Mao and Lenzi, 2007; Rainato et al., 2017) and the Jordan and Meshushim rivers in Israel (Inbar and Schick, 1979).
The Rio Cordon and its catchment (5 km^2) are situated in the Dolomites of Italy. The sediment characteristics are: D_{10} = 26 mm (where D_{10}=diameter for which 10 percent of the particles are finer), D_{50} = 100-120 mm and D_{90} = 450 mm. The ratio D_{90}/D_{10} is 20 to 30 (widely graded mixture). The steep channel width in a typical cross section just upstream of the measurement station varies from 5 to 7 m during flood conditions. The measurement station consists of an inlet flume, an inclined grid where the separation of coarse particles takes place, a storage area for coarse sediment deposition, and an outlet flume to return water and fine sediment to the stream. An exceptional flood event occurred on 14 September 1994, see Table 4. The mean flow velocity was about 3 m/s and the measured bed load transport was about 14 kg/(m s).
Inbar and Schick (1979) have studied the bed load transport during flash floods in the upper Jordan River and the Meshushim River in Israel, see Table 4. The Jordan River drains an area of 1590 km^2 into Lake Kinneret. Peak winter flow approximates 100 m^3/s. The highest flow during the 43 years recorded data is 214 m^3/s. Bed load transport is about 1% to 2% of the total sediment yield and occurs mainly during flows that exceed 60 m^3/s (flow velocity > 1.5 m/s).
The measured bed load transport data and the equations of MPM and Cheng are shown in Fig. 3. The original MPM-equation shows good agreement with the MPM-flume data for α = 1.5, which means that the effective grain roughness of the coarse sediment bed in the MPM-flumes can be represented by k_s = 1.5 D_{50}. The original MPM equation shows good agreement with the field data for θ-values in the range of 0.06 to 0.08. The field data for θ < 0.035 are strongly underpredicted by both equations. Two explanations may be possible for this discrepancy. The measured bed load transport values which are derived from post flood deposits may have been "polluted" by the presence of much finer sediment transported as suspended load. It is known

that steep coarse bed rivers generally have a very wide particle size distrution with $D_{90}/D_{10} \cong 20$ to 30 and, thus, a relatively large finer fraction. Furthermore, the depth-averaged velocity may have been underestimated by the field workers during the flash flood events.

The computed bed load transport rates based on the MPM-equation are zero for $\theta < 0.047$, whereas the measured transport values of Paintal (1971) clearly show that bed load transport occurs for θ-values in the range of 0.02-0.047. The relatively high field measured bed load transport values of the Israeli rivers for θ-values in the range of 0.01-0.032 may be questionable (due to presence of suspended load deposits). The results show that the approach of MPM fails for conditions around the threshold condition (θ_{cr} = 0.03 to 0.05). The equation of Cheng shows fairly good agreement with the measured bed load transport rates of Paintal (1971). Van den Bos et al. (2010) have found that the approach of Paintal (1971) and Cheng (2002) also can be used for coastal conditions with combined current and wave conditions.

In the following section the Cheng (2002)-equation is used to estimate the loss of rocks from a bed protection system if the hydrodynamic conditions are slightly above the critical conditions.

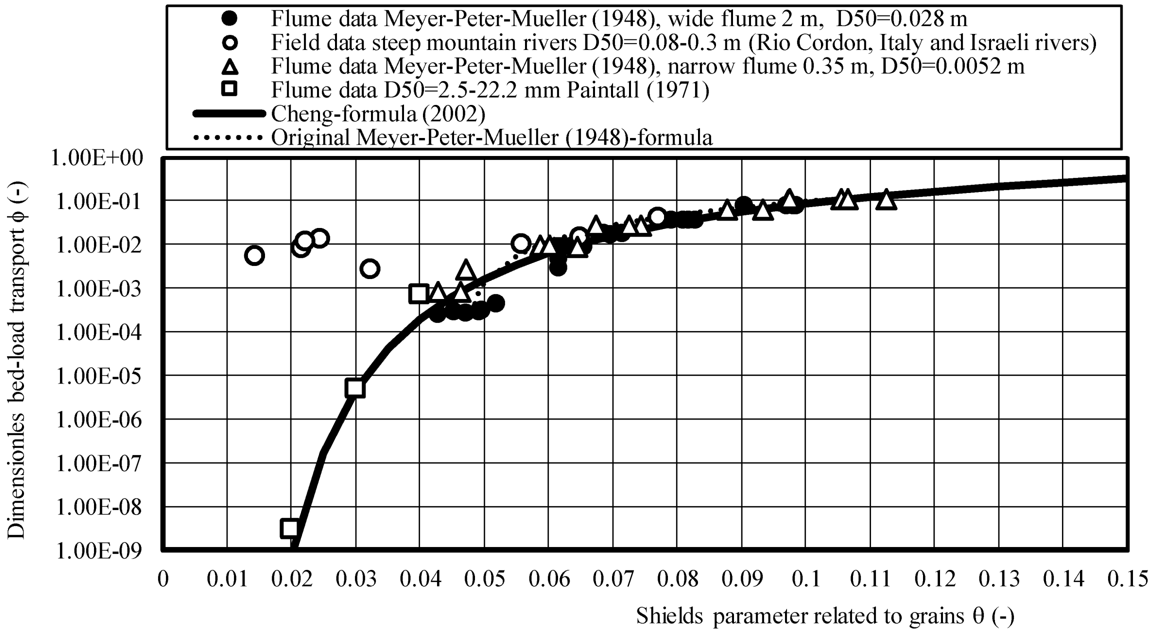

Fig. 3. Dimensionless bed load transport at low values of the Shields-parameter

Table 4. Bed load transport data of cobbles, boulders, and rocks for field conditions

River	Event	Dia meter (m)	Dis charge (m^3/s)	Width (m)	Depth (m)	Slope (-)	Mean velocity (m/s)	Mobility number (-)	Bed load transport (kg/(m s)
Rio Cordon	14 Sep. 1994	0.11	10.4	7	0.5	-	3	0.075	14
Jordan	22-25 Jan. 1969 (72 hrs)	0.3	180-214	43	1.4	0.035	3.3	0.032	4.8
	21 Jan. 1974 (10 hours)	0.1	91-98	40	1.2	0.035	2.0	0.022	2.7
	21 Jan. 1974 (10 hours)	0.1	91-98	24	1.7	0.03	2.3	0.024	4.5
	10 Feb. 1975 (6 hours)	0.08	55-60	34	1.1	0.035	1.5	0.014	1.3
	10 Feb. 1975 (6 hours)	0.08	55-60	19	1.5	0.03	2.0	0.022	2.7
Meshushim	22 Jan. 1969 (3 hours)	0.3	300	31	2.0	0.03	4.8	0.056	17.6
	22 Jan. 1969 (10 hours)	0.2	200	26	1.7	0.03	4.5	0.065	13.8

4. Large cobles and rocks used as bed protection

4.1. General

The design of a bed protection layer consisting of loose cobbles, boulders, and rocks (rubble mound) requires knowledge of the stability and movement (as bed load) of very coarse sediment materials. The design of stable rock size D_{50} can be determined by Eq. 7. It is assumed that the coarse bed protection layer is constructed on top of a filter layer and/or a geotextile to prevent the erosion of fine sediments from beneath and the sinking of the coarse units into the bed.
Two types of bed protection can be designed: static or dynamic protection. Static bed protection means that the rocks are fully stable under design conditions without any damage/movement. Dynamic bed protection is obtained if some movement (or damage) is acceptable allowing use of smaller rock sizes. This approach requires the inclusion of a damage/movement level or damage parameter. Various applications are given to demonstrate the applicability of the proposed equations (Section 4.3).

4.2. Damage equations

A damage estimate (loss of rocks) can be obtained if the bed load transport at low mobility parameters in the range of 0.01 to 0.05 can be computed by an accurate expression (Section 3). Using Equation 9 of Cheng (2002), the bed load tranport in terms of mass can be converted into the number of moving rocks per unit width (m) and time (s) by using the mass of one rock $M_{rock} = (1/6)\ \pi\ \rho_s\ D_{50}^3$ resulting in:

$$N_{mr} = \frac{13\ \rho_s\ (s-1)^{0.5}\ g^{0.5}\ D_{50}^{1.5}\ \theta^{1.5}\ \exp(\frac{-0.05}{\theta^{1.5}})}{\left(\frac{1}{6}\right)\pi\ \rho_s\ D_{50}^{3}} \qquad (10a)$$

$$N_{mr} = 25\ (s-1)^{0.5} g^{0.5} D_{50}^{-1.5} (r\ \theta_{cr,shields})^{1.5}\ \exp\{\frac{-0.05}{(r\theta_{cr,shields})^{1.5}}\} \qquad (10b)$$

where
N_{mr} = number of moving rocks per m width and per s at critical conditions (per day by multiplication with 86400 s); and
$\theta = r\ \theta_{cr,shields}$ = mobility parameter at critical conditions.

Equations 10a,b can be used to get an estimate of the number of moving rocks during a given period.

A damage parameter which is often used to express the damage for a bed protection is defined as (CIRIA/CUR/CETMEF, 2007):

$$S_d = \frac{A_e}{D_{50}^2} = \Delta t\ \left[\frac{1}{1-\varepsilon}\right]\left[\frac{V_{rock}}{D_{50}^2}\right] N_{mr} = \left(\frac{\pi}{6(1-\varepsilon)}\right)\Delta t\ D_{50} N_{mr}\ \cong\ \Delta t\ D_{50} N_{mr} \qquad (11)$$

where
A_e= eroded area (including pores) per unit width in time period Δt;
Δt = time period considered (usually 5,000 to 10,000 waves or about 1 day of storm; Δt in days if N_{mr} in -/(m day)),
ε = porosity factor ($\cong$ 0.45); and
V_{rock} = volume of a single rock particle.
The factor $(\pi/6)/(1-\varepsilon)$ is asumed to equal to 1.

The number of rocks moving out of the bed protection area in a given time period can be seen as damage requiring maintenance. The damage percentage in a given time period can be computed as the ratio of the number of rocks moving away (loss) and the total number of rocks available.

The loss of rocks from a bed protection area with length, L_{bp}, and thickness, $\delta_{bp} = \alpha_{bp} D_{50}$, can be determined, as follows:

Volume of bed protection per unit width: $V_{bp} = L_{bp}\ \delta_{bp}$

Number of rocks in bed protection area: $N_{bp} = \frac{(1-\varepsilon)\ L_{bp}\ \alpha_{bp}\ D_{50}}{\left(\frac{\pi}{6}\right) D_{50}^3} = \frac{6\ (1-\epsilon)\ \alpha_{bp}\ L_{bp}}{\pi\ D_{50}^2} \cong \frac{2\ (1-\varepsilon)\ \alpha_{bp}\ L_{bp}}{D_{50}^2}$

Number of rocks moving out of bed protection area during the lifetime: $N_{loss} = N_{mr}\ T_{event} T_{life}$

The loss coefficient can be determined, as:

$$P_{loss} = \frac{N_{mr}\ T_{event}\ T_{life}}{N_{bp}} = \frac{N_{mr}\ T_{event}\ T_{life}}{2\ \alpha_{bp}\ (1-\varepsilon)\ L_{bp}\ D_{50}^{-2}} \qquad (12)$$

where
L_{bp}= length of bed protection area (normal to flow or waves);
$\alpha_{bp} \cong$ 2 to 3;
T_{event} = duration of extreme events per year (in days per year); storm event or river flood event; and
T_{life} = lifetime of structure (years).

Equation 10b depends on two parameters: the r-coefficient and D_{50}. The r-coefficient which is an input parameter, can be used to define the amount of acceptable damage. A relatively small r-value (r = 0.3 or 0.4) can be used if static protection (without damage) is preferred for design conditions. A dynamic protection accepting some damage will be obtained for larger r-values.

To verify Eqs. 5, 9, and 10a for combined current and wave conditions (low mobility range), the laboratory test results of Bijman (2000) are used. Bijman (2000) did flume experiments with current and waves over a horizontal bed protection of granular material (D_{50} = 0.0055 m). Measured and computed results for four representative tests with waves of about 0.13-0.15 m and currents of 0.35 to 0.65 m/s are listed in Table 5. Computed results are based on: $k_s = 1.5D_{50}$ and $\gamma_{str} = 1$ (no structures). Very reasonable agreement between computed and measured results can be observed. The computed number of moving stones are of the right order of magnitude.

Table 5. Measured and computed moving stones along horizontal bed protection in conditions with combined current and waves; D_{50} = 0.0055 m; mass 1 stone = 0.000224 kg; test duration Δt = 3960 s (Bijman 2000)

Test	**Water depth (m)**	**Wave height and period (m), (s)**	**Depth-averaged current (m/s)**	**Measured bed load transport (kg/(m s))**	**Number of moving stones per m width during the test duration**	
					Measured	**Computed**
BM2	0.286	0.154; 1.1	0.35	0	0	<<1
BM4	0.317	0.151; 1.1	0.42	$0.034\ 10^{-6}$	0.6	<<1
BM18	0.279	0.142; 1.1	0.57	$1.3\ 10^{-6}$	23	10
BM29	0.284	0.134; 1.1	0.65	$2.3\ 10^{-6}$	40	120

As an example, the number of moving rocks (per m width and per day; Δt = 86400 s) based on Eq. 10a is shown in Fig. 4 for a particular case with rocks in the range of D_{50} = 0.02 to 0.5 m and current velocities in the range of 1 to 7 m/s (no waves). The water depth is equal to 5 m. The input parameters are α = 2, γ_{str} = 1.
Assuming almost no movement for $N_{mr} < 0.0001$ (per m and per day), the critical depth-mean velocities for static protection are: $u_{cr} \cong 1.3$ m/s for D_{50} = 0.02 m to $u_{cr} \cong 4.2$ m/s for D_{50} = 0.5 m in a flow with depth of 5 m. Accepting some movement and damage with N_{mr}=1 per m and per day, the critical depth-mean velocities increase to $u_{cr} \cong 1.5$ m/s for D_{50} = 0.02 m and $u_{cr} \cong 5$ m/s for D_{50} = 0.5 m.
It is noted that Fig. 4 represents a computational exercise which cannot be justified directly because field data on the loss of rocks is not available. However, the underlying equations of critical velocity (Eq. 7) and bed load transport of rocks (Eq. 9) have been justified based on field data (see Sections 2 and 3).

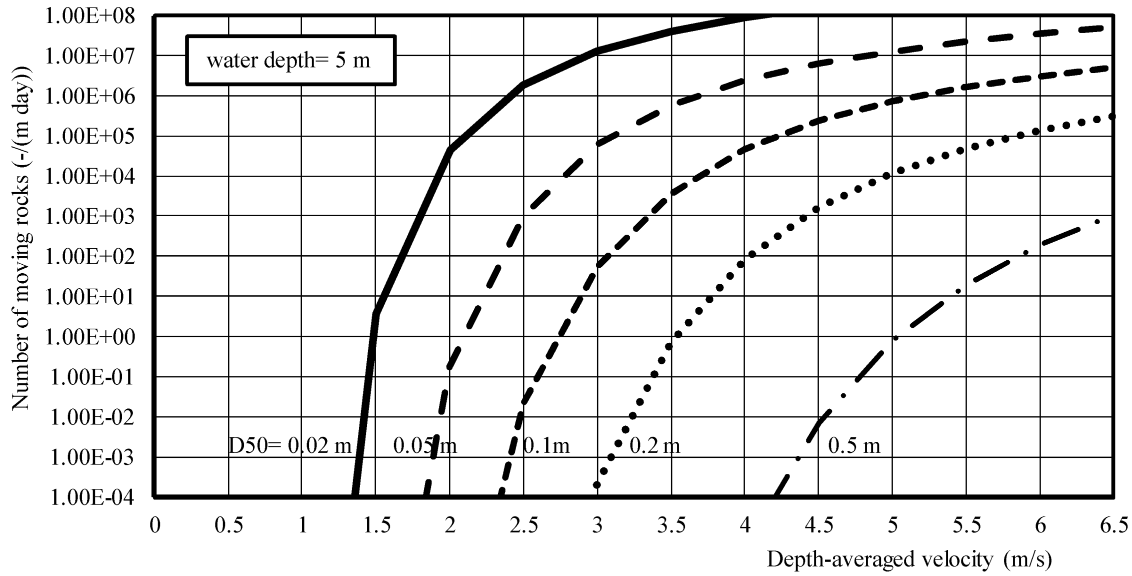

Fig. 4. Number of moving rocks (N_{mr}) of horizontal bed protection in current conditions (h = 5 m)

4.3. Practical applications

4.3.1. Rock protection to stabilize channel bed in river flow

Equation 7, which is justified in Section 2 based on field data in current conditions, has been used to produce a design graph for horizontal bed protection in water depths of h_o = 3 to 20 m and depth-averaged velocities u_c = 1 and 5 m/s.
The thickness of the protection layer is set to δ_{bp} = 0.5 m.
The effective water depth is: $h_{bp}=h_o-\delta_{bp}$.
Other parameters are:
density of seawater = 1020 kg/m^3; density of sediment = 2650 kg/m^3;
α = 2, $\theta_{cr,o}$= r $\theta_{cr,shields}$ with r = 0.5 and $\theta_{cr,shields}$ = 0.05;
γ_{str} = 1 (no additional velocity-turbulence enhancement due to bed protection layer) and
γ_s = safety factor = 1. The computed results are shown in Fig. 5.

The results clearly show that the rock diameter decreases for increasing water depth at the same depth-averaged velocity, because the bed-shear stress decreases with increasing water depth (less flow resistance). In the case of a bed protection with rock size D_{50} = 0.1 m, thickness δ_{bp} = 0.5 m, $\alpha_{bp} = \delta_{bp}/D_{50}$ = 5, length L_{bp} = 50 m, and porosity ε = 0.45 in a flow with depth of h = 5 m and current velocity u_c = 2.5 m/s, the number of moving rocks per day is N_{mr} = 0.02 (Fig. 4) and S_d= 0.002 (for 1 day).

The loss coefficient of rocks for an extreme event time of 30 days per year (with velocity of 2.5 m/s) and a lifetime of 50 years for the bed protection layer is:
P_{Loss} = [0.02x30x50]/[2x5x(1-0.45)x50x(0.1)$^{-2}$]= 30/27500= 0.0011 (0.11%) during the lifetime of the stucture.

The thickness of the protection layer can be reduced to 0.3 m resulting in a loss coefficient of about 0.2%. In both cases (δ_{bp} = 0.5 m or 0.3 m), the damage is so low that static bed protection is obtained.

Using: rock size = D_{50} = 0.08 m and δ_{bp} = 0.5 m, the number of moving rocks per m per day goes up to N_{mr} = 1 (50 times larger, Fig. 4) and S_d = 0.08 for 1 day. The loss coefficient goes up by a factor of 50 to about 6%, which may be acceptable (dynamic bed protection for D_{50} = 0.08 m).

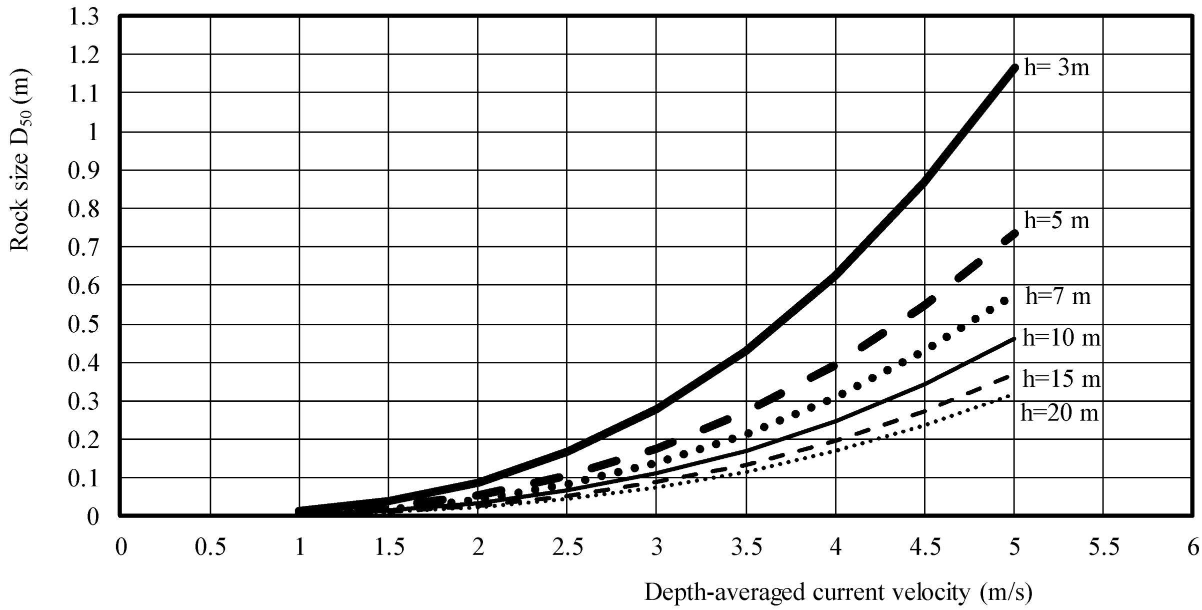

Fig. 5. Design graph (r = 0.5, γ_{str} = 1) for horizontal bed protection in current conditions

4.3.2. Rock bed protection near quay mooring in a harbor

Traditionally, armor layers of rocks have been used for berth protection against ship propeller velocities and ship-induced waves. The size of conventional vessels with draughts up to 15 m and propeller diameters ranging up to 8 m is continually increasing creating jet flows with relatively high velocities, while the bottom clearances also are reduced. The combination of larger propeller jet flows and a reduction in bed clearance has created higher levels of bed impact. Transverse bow and stern thrusters with diameters ranging from 1 to 3 m are used to aid berthing and unberthing. During berthing, the propulsion water jets can have exit velocities in the range of 10 to 15 m/s resulting in scour of the bed (Hawkswood et al. 2014). Bed protection generally consists of two layers of rock armor units upon a bedding/filter layer. Fig. 6 shows the required rock diameter range as a function of the propeller-induced near-bed velocity based on experimental research at BAW (2005). Rock diameters larger than 1 m are required for velocities > 4 m/s, which often is impractical. Large rock diameters lead to an increase of the span and embedment heights of the quay walls with major cost increase effects.

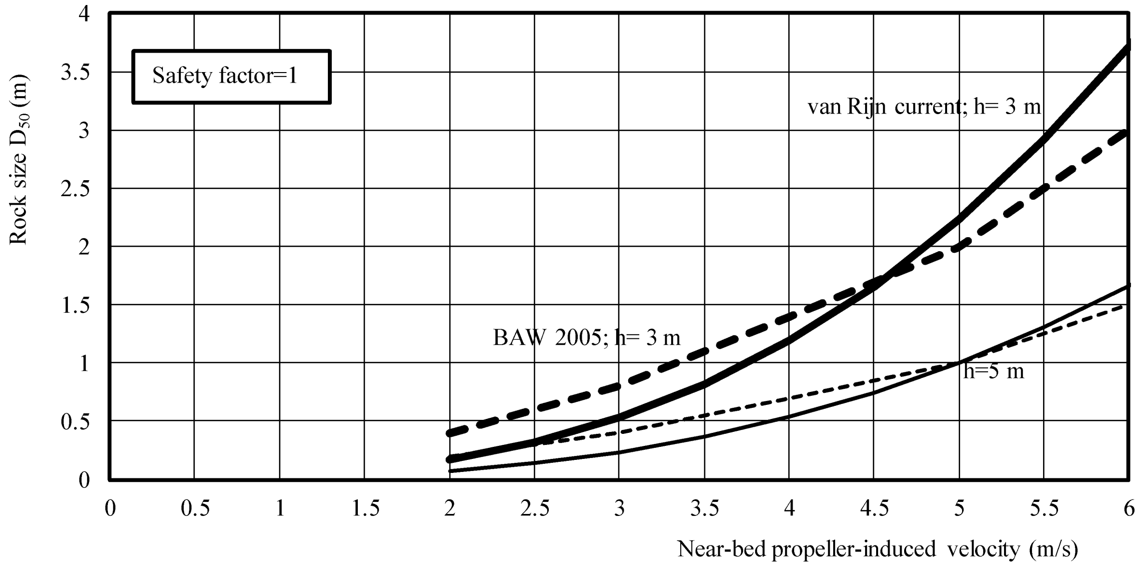

Fig. 6. Rock size for bed protection layers at berthing sites

Equation 7 has been used to estimate the stable rock size against near-bed velocities generated by ship propellers. It is assumed that the propeller axis is about 3 to 5 m above the bottom and that a boundary layer flow (with layer thickness h = 3 to 5 m) is generated locally. The input parameters are: boundary layer height h= 3 and 5 m, mean flow velocity in the boundary layer u_c = 2 to 6 m/s, bed roughness coefficient α = 1, Shields-reduction coefficient r = 0.5, Shields mobility number $\theta_{cr,shields}$ = 0.05, turbulence enhancement factor γ_{str} = 1.2. The computed results are shown in Fig. 6 and are in reasonable agreement with the experimental BAW-results. These results justify the validity of Eq. 7 and confirm that excessively large rock diameters are required to obtain stable rocks in conditions with velocities > 4 m/s close to the bottom.

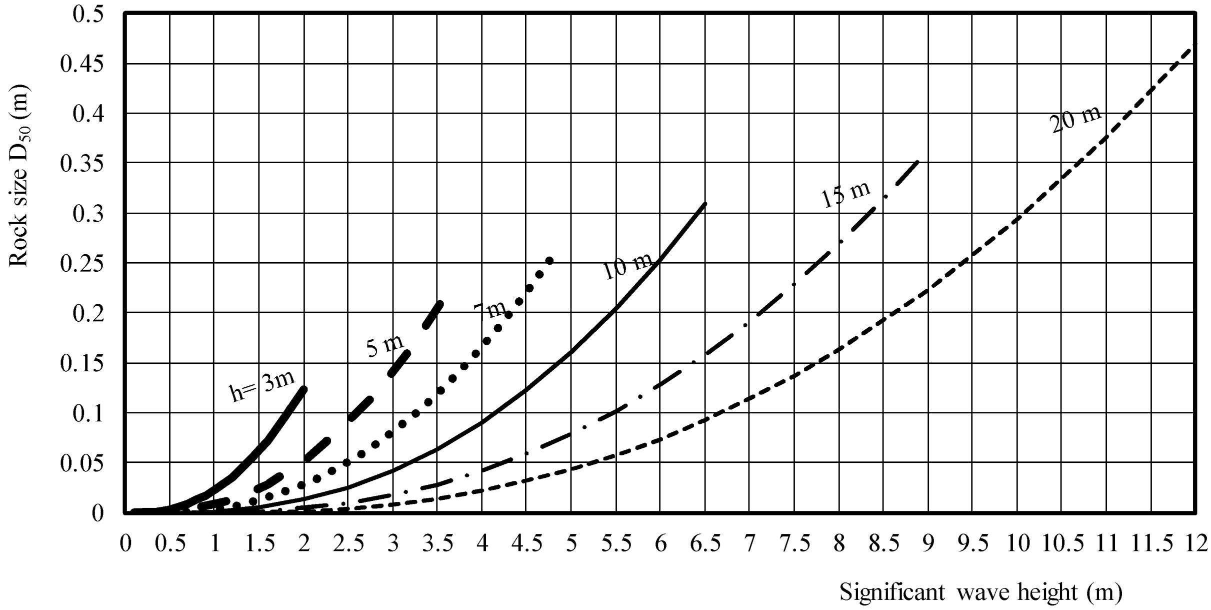

Fig. 7. Design graph (r = 0.5; γ_{str} = 1) for horizontal bed protection in wave conditions

4.3.3. Rock protection to stabilize seabed

Equation 7, which is justified in Section 2 based on field data in sea conditions, has been used to produce a design graph for horizontal bed protection in water depths of h = 3 to 20 m and significant wave heights between H_s = 0.1 and 12 m. The wave period T_p is given by the relation $T_p = 5\ H_s^{0.4}$ (North Sea wave climate). The thickness of the protection layer is set to δ_{bp} = 0.5 m. The effective water depth is $h_{bp} = h_o - \delta_{bp}$. Other parameters are: density of seawater = 1020 kg/m^3; density of sediment = 2650 kg/m^3; γ_s = 1 = safety factor, γ_{str} = 1, α = 2, r = 0.5 and $\theta_{cr,shields}$ = 0.05. The computed results are shown in Fig. 7. For example: h = 17 m and H_s = 4.6 m (T_p = 9.2 s) yields: D_{50} = 0.048 m for r = 0.5 and N_{mr} = 10 rocks/(m day). This latter parameter can be reduced to N_{mr} = 0.033 by using a larger rock size D_{50} = 0.066 m (r = 0.4).

4.3.4. Rock protection near monopiles in coastal seas

Bed protection around monopiles of wind mills in coastal waters have been intensively studied. Equation 7 can be used to design the rock size of bed protection around a monoplile (see Fig. 8) provided that the effect of the structure on the local velocity field is known with sufficient accuracy. This effect is represented by the γ_{str}-coefficient (range of 1 to 1.5) of Eq. 7.

Miles et al. (2017) have studied the current and wave fields around a monopile at a scale of 1 to 25 in a wave-current basin. The waves are normal to the current. Based on their measured data, it can be concluded that:

- the most significant current-related wake region downstream of the pile has a length of 5D_{pile} with D_{pile} = pile diameter; the total distance of disturbed velocities is about 10D_{pile}; the maximum turbulent velocities occur at a distance of 2D_{pile} downstream of the pile center; the maximum standard deviation of the instantaneous velocities at that location is about σ_U = 0.7 $u_{c,o}$ with $u_{c,o}$ = depth-averaged current velocity upstream of the pile;
- the maximum velocity at both sides of the pile is about $u_{c,local}$ = 1.35 $u_{c,o}$ at 0.75D_{pile} from the pile center (normal to main current direction);
- the wave-related influence zone with disturbed orbital velocities is about 3D_{pile} on both sides of the pile (waves only); the maximum orbital velocity in the influence zone is about $U_{w,local}$ = 1.85$U_{w,o}$ with $U_{w,o}$= (undisturbed) near-bed orbital velocity outside the influence zone.

De Vos et al. (2012) have done experimental work in a wave-current basin on a circular bed protection around a monopile foundation. The overall diameter of the circular bed protection area is about 5D_{pile}. The thickness of the bed protection is 2.5 to 3D_{50}. Various sizes of angular protection material have been used: D_{50} = 3.5, 5 and 7.2 mm. The protection material was placed on top of the sand bed (D_{50} = 0.1 mm).

Ten results covering the test range (Table 6) have been used to analyze the γ_{str}-parameter of Eq. 7 using: s= 2.6, δ_{bp} = 0.02 m = thickness of protection layer, α = 2, r= 0.5, $\theta_{cr,shields}$ = 0.05, and γ_s = 1. The γ_{str}-parameter represents the effect of the monopile on the enhancement of the local depth-averaged velocity and the additional turbulence generated by the pile structure. The results are listed in Table 6 (last two columns).

Table 6. Stability test results of circular bed protection around a monopile

Test	Stone size (mm)	Number of waves (-)	Water depth (m)	Depth-mean velocity u_c (m/s)	Significant wave height H_s (m)	Peak wave period T_p (s)	Dimensionless parameter related to scour of stones S_{3d} (-)	Computed	
								γ_{str} (-)	S_{damage} (-)
6	3.5	5000	0.4	0.08	0.135	1.42	0.60; D.L.=3	1.2	<0.1
14	3.5	5000	0.4	0.164	0.088	1.42	0.24; D.L.=1	1.6	<0.1
19	3.5	3000	0.4	0.163	0.130	1.71	0.94; D.L.=3	1.1	<0.1
50	5.0	5000	0.4	0.224	0.109	1.71	0.64; D.L.=3	1.4	<0.1
52	5.0	3000	0.4	0.315	0.058	1.71	1.21; D.L.=4	1.6	0.15
53	7.2	5000	0.4	0.156	0.145	1.71	0.35; D.L.=2	1.4	<0.1
54	7.2	5000	0.4	0.221	0.121	1.42	0.19; D.L.=2	1.6	<0.1
73	7.2	3000	0.4	0.066	0.151	1.71	0.98; D.L.=3	1.4	<0.1
77	7.2	3000	0.4	0.203	0.122	1.42	0.99; D.L.=3	1.6	<0.1
84	5.0	3000	0.4	0.214	0.135	1.42	0.40; D.L.=2	1.3	<0.1

D.L.=Damage Level; D.L. = 1 = no movement; D.L. = 2 = very limited movement of stones (S_{3d} = 0.3-0.5); D.L. = 3 (S_{3d} = 0.5-1); D.L. = 4 = failure

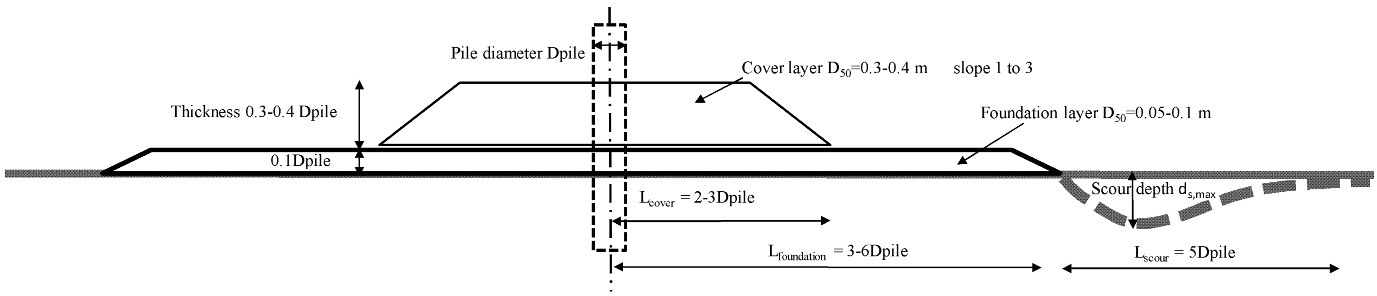

Fig. 8. Bed protection layers around a monopile

The computed γ_{str}-values vary in the range 1.1 to 1.6 or γ_{str} = 1.4±0.2 (about 15% variation). Miles et al. (2017) have found that the local velocity increase due to the presence of the pile is about 35%, which is in agreement with a velocity enhancement coefficient of γ_{str} = 1.4.
The construction of a monopile in the seabed requires the protection of the local bed around the pile by a cover rock layer, see Fig. 8. Often, the protection layer consists of a foundation layer and a cover layer. The length of the foundation layer is determined by the acceptable scour depth. The scour depth is on the order of $d_{s,max} \cong D_{pile}$ for $L_{foundation}$= $3D_{pile}$ and $d_{s,max} \cong 0.1D_{pile}$ for $L_{foundation} = 6D_{pile}$ (Whitehouse et al., 2008).

De Vos et al. (2012) have defined a field example case with the following values: D_{pile} = 5 m, water depth h= 20 m, current u_c = 1.5 m/s, significant wave height H_s = 6.5 m, peak wave period T_p = 11.2 s, density seawater ρ_w = 1020 kg/m^3, thickness of protection layer δ_{bp} = 2 m. The expression proposed by the De Vos et al. (2012) yields: D_{n50} = 0.34 m. Equation 7 has also been used for the example of De Vos et al. (2012). Using: effective water depth $h_{bp} = h_o - \delta_{bp}$ = 20-2 = 18 m, r = 0.5, $\theta_{cr,shields}$ = 0.05 and α = 2, the rock size is: D_{50} = 0.36 m and $N_{moving\ rocks}$ = 0.5 moving rocks/(m day), (damage $S_d \cong 0.18$ for 1 day) for γ_{str} = 1.4. Thus, Eq. 7 yields almost the same result as that of De Vos et al. (2012), which is another justification of Eq. 7.

5. Conclusions

Cobbles, boulders, and rocks often are used as a bed protection layer or armor layer near a structure to protect the underlying sand bed against erosion by combined current and waves. The design of a bed protection layer consisting of loose rocks (rubble mound) requires knowledge of the stability and movement (as bed load) of very coarse materials. If some movement (or damage) is acceptable, the rock diameter can be designed to be smaller. This paper has addressed the stability and movement of very coarse materials (cobbles, boulders, and rocks) based on the concept of the critical Shields mobility number related to a prescibed damage level. General equations for the design of the rock size of a bed protection layer (including damage) in conditions with current with or without waves are proposed. The proposed equations are valid for rock sizes up to 3 m based on testing with field data. The damage parameter is derived from the bed load equation of Cheng (2002), which is found to be valid for relatively small Shields mobility numbers.

The following conclusions are drawn:

1. The material size of bed protection layers consisting of cobbles, boulders, and rocks can be computed using the concept of the Shields mobility number, both in current, waves and combined current plus waves.
2. The critical Shields number can be related to a prescribed damage level, which is expressed by the r-coefficient being a correction parameter in the range of r = 0.4-0.5 to the original Shields'curve value of 0.05 for coarse granular materials. Smaller r-values yield larger rock sizes.
3. The most realistic critical Shields number for stable coarse materials is $\theta_{cr} \cong 0.02$ to 0.025 (r = 0.4 to 0.5).
4. The bed load transport of rocks with diameters of 0.1 to 0.5 m for Shields numbers > 0.05 can be very well described by the original Meyer-Peter and Mueller bed load transport equation.
5. The bed load transport of rocks for Shields numbers in the range of $\theta = 0.01$ to 0.04 can be described by the equation Cheng (2002). This equation can be used to estimate the damage of a rock-type bed protection in extreme conditions.
6. The effect of the structure on the near-bed velocity and turbulence field can be taken into account by a velocity enhancement coefficient (γ_{str}), which has been found to be in the range of 1 to 1.6.

The overall error of the proposed method cannot be very accurately determined as independent field data are lacking. Almost all (scarcely) available field data have been used for calibration of the method. As an independent check, some laboratory data of Bijman (2000) related to a horizontal bed protection in current plus wave conditions has been used, showing very reasonable results (Table 5). Furthermore, the calibration coefficients involved are found to be fairly constant ($\alpha \cong 1.5$ to 2 and $r \cong 0.4$ to 0.5) for very different cases. The velocity enhancement coefficient (γ_{str}) varies from case to case depending on the turbulence structure. The range of the cases considered herein suggests values up to 1.6. Larger values can be used for cases with exceptional turbulence levels.

6. Acknowledgements

Bernard Malherbe of Jan De Nul Dredging (Belgium) is gratefully acknowledged for his stimulating discussions on the critical movement of cobbles, boulders and rocks.

7. References

Attal, M., & Lavé, J., (2009). Pebble abrasion during fluvial transport. *Journal of Geophysical Research*, *114, F04023*

Bundesanstalt für Wasserbau (BAW), (2005). *Principals for the design of bank and bottom protection for inland waterways, Bulletin 85*, Karlsruhe, Germany

Bijman, W., (2000). *Transport of granular material by waves plus currents. MSc Thesis*, Department of Civil Engineering, Delft University of Technology, Delft, The Netherlands (in Dutch)

Cheng, N.S., (2002). Exponential formula for bed load transport. *Journal of Hydraulic Engineering*, *128 (10)*, 942-946.

Cheng, N.S., Liu, X., Chen, X., & Qiao, C., (2016). Deviation of permeable coarse-grained boundary resistance from Nikuradse's observations. *Water Resources Research, 52 (2)*, 1194-1207

Construction Industry Research and Information/CUR Building of Infrastructure/Center d'Etudes Techniques Maritimes et Fluvials (CIRIA/CUR/CETMEF), (2007). *Manual; the use of rock in coastal and shoreline engineering.* London

Crickmore, M.J., Waters, C.B., & Price, W.A., (1972). The measurement of offshore shingle movement. *Proceedings 13th International Conference Coastal Engineering ICCE 1972*, Vancouver, Canada

Deltares. (1972). *Systematic investigation of two-dimensional and three-dimensional scour.* Report M648/M893, Delft, The Netherlands (in Dutch)

De Vos, L., De Rouck, J., Troch, P., & Frigaard, P., (2012). Empirical design of scour protections around monopile foundations, Part 2: Dynamic approach. *Coastal Engineering 60*, 486-498

Fahnestock, R.K., (1963). *Morphology and hydrology of a glacial stream White River, Mount Rainier. U.S. Geological Survey Professional Paper 422-A*, Washington, DC, U.S.

Graf, W. H., (1971). *Hydraulics of sediment transport*. New York: McGraw-Hill

Hall, A.M., (2010). Storm wave currents, boulder movement and shore platform development: a case study from East Lothian, Scotland. *Marine Geology 283*, 98-105

Hansom, J.D., Barltrop, N.D.P., & Hall, A.M., (2008). Modelling the processes of cliff-top erosion and deposition under extreme storm waves. *Marine Geology, 253*, 36-50

Hawkswood, M.G, Lafeber, F.H., & Hawkswood, G.M., (2014). Berth scour protection for modern vessels. *Proceedings PIANC World Congress San Francisco*, U.S.

Helley, E.J., (1969). *Field measurement of the initiation of large bed particle motion in Blue Creek near Klamath, California. U.S. Geological Survey Professional Paper 562-G*, Washington, DC, U.S.

Hofland, B., (2005). *Rock and roll; turbulence-induced damage to granular bed protections. Doctoral Thesis.* Delft University of Technology, Delft, The Netherlands

Hudson, R.Y., (1958). *Design of quarry stone cover layers for rubble mound breakwaters. U.S. Army Engineer Waterways Experiment Station, Research Report No. 2-2*. Vicksburg, MS, U.S.

Inbar, M., & Schick, A.P., (1979). Bed load transport associated with high stream power, Jordan River, Israel. *Proceedings of the National Academic Science U.S., 76, (6)*, 2517-2525

Lenzi, M.A., (2004). Displacement and transport of marked pebbles, rocks and boulders during floods in a steep mountain stream. *Hydrological processes, 18, (10)*, 1899-1914.

Lenzi, M.A., Mao, L., & Comiti, F., (2006). Effective discharge for sediment transport in a mountain river. *Journal of Hydrology, 326*, 257-276

Mao, L., & Lenzi, M.A., (2007). Sediment mobility and bed load transport conditions in an alpine stream. *Hydrological processes, 21, (10)*, 1882-1891

Maynord, S.T., (1978). *Practical riprap design. U.S. Army Engineer Waterways Experiment Station, Miscellaneous Paper H-78-7*, Vicksburg, U.S.

Meyer-Peter, E., & Mueller, R. (1948). Formulas for bed load transport. *Proceedings of the International Association for Hydraulic Research, 2nd meeting (pp. 41-64)*, Stockholm

Miles, J., Martin, T., & Goddard, L., (2017). Current and wave effects around wind farm monopile foundations. *Coastal Engineering 121*, 167-178

Mueller, E.R., Pitlick, J., & Nelson, J.M., (2005). The variation in the reference Shields stress for bed load transport in gravel-bed streams and rivers. *Water Resources Research, 41, w04006*

Neill. C.R., (1968). *A re-examination of the beginning of movement for coarse granular bed materials.* Technical Report, Hydraulics Research Station Wallingford, UK.
Nikuradse, J., (1932). Gesetzmässigkeiten der Turbulente Strömung in glatten Rohren. Forschungsarbeiten aus dem Gebiete des Ingenieurwesens. *Verein Deutscher Ingenieure, Forschungsheft 356*, Berlin, Germany
Nikuradse, J., (1933). Strömungsgesetze in rauhen Rohren. Forschungsarbeiten aus dem Gebiete des Ingenieurwesens, *Verein Deutscher Ingenieure, Forschungsheft 361*, Berlin, Germany
Paintal, A.S., (1971). Concept of critical shear stress in loose boundary open channels. *Journal of Hydraulic Research, 9 (1), 91-113*
Pilarczyck, K.W., (1998). *Dikes and revetments.* Rotterdam: Balkema
Rainato, R., Mao, L., Garcia-Rama, Picco, L., Cesca, M., Vianello, A., Preciso, E., Scussel, G.R., & Lenzi, M.A., (2017). Three decades of monitoring in the Rio Cordon instrumented basin: Sediment budget and temporal trend of sediment yield. *Geomorphology, 291*, 45-56
Schiereck, G.J., & Verhagen, H.J., (2016). *Introduction to bed, bank and shore protection*. Delft, The Netherlands: Delft Academic Press.
Shields, A., (1936). *Anwendung der Ähnlichkeitsmechanik und der Turbulenz Forschung auf die Geschiebebewegung.* Mitteilung der Preussischen Versuchsambt für Wasserbau und Schiffbau, Heft 26, Berlin
Soulsby, R., (1997). *Dynamics of marine sands.* London: Thomas Telford.
Tørum, A., Arntsen, O.A., & Kuester, C., (2010). Stability against waves and currents of gravel rubble mounds over pipelines and flat gravel beds. *Proceedings 32nd International Conference on Coastal Engineering ICCE 2010*, Sjanghai, China
Turowski, J.M., Yager, E.M., Badoux, A., Rickenmann, D., & Moinar, P., (2009). The impact of exceptional events on erosion, bed load transport and channel stability in a step-pool channel. *Earth Surface Processes and Landforms, 34*, 1661-1673
Van den Bos, J.P., Verhagen, H.J.,& Olthof, J., (2010). Low-mobility transport of coarse-grained bed material under waves and currents. *Proceedings 32nd International Conference on Coastal Engineering ICCE 2010*, Sjanghai, China
Van Rijn, L.C., (1993). *Principles of sediment transport in rivers, estuaries and coastal seas*, Amsterdam: Aquapublications
Van Rijn, L.C., (2006). *Principles of sediment transport in rivers, estuaries and coastal seas*, Part II: Supplement 2006, Amsterdam: Aquapublications
Van Rijn, L.C., (2011). *Principles of fluid flow and surface waves in rivers, estuaries, seas and oceans.* Blokzijl (The Netherlands): Aquapublications.
Verhagen, H.J., & Jansen, L., 2014. *Ratio of stone diameter and nominal diameter. Communications on Hydraulic and Geotechnical Engineering 2014-01*, Delft University of Technology, Delft, The Netherlands
Whitehouse, R., Harris, J., Sutherland, J., & Rees, J., (2008). An assessment of field data for scour at offshore wind turbine foundations. *Proceedings Fourth International Conference on Scour and Erosion*, Tokyo.
Yalin, M.S., (1977). *Mechanics of sediment transport*. Oxford: Pergamon Press